Mirror-image Dependence: Targeting Enantiomeric G-quadruplex DNA by 10 Pairs of Triplex Metallohelices

Chuanqi Zhao,[a] Hualong Song,[b] Peter Scott,[b] Andong Zhao,[c] Hisae Tateishi-Karimata,[d] Naoki Sugimoto,[d] Jinsong Ren,[a] and Xiaogang Qu*,[a]

Abstract: DNA chirality is the fundamental issue for design of DNA-targeted chiral drugs and DNA-based chiral devices. Natural D-DNA and L-DNA are mirror-image counterparts. However, due to the inherent flexibility and conformation diversity of DNA, it is still not clear how enantiomeric compounds to recognize D-DNA and L-DNA. Are their recognitions following mirror-image dependence? Herein, taken G-quadruplex (G4) DNA as an example which has diverse conformations and distinct biofunctions, 10 pairs of iron triplex metallohelices binding to D- and L-G4 DNA have been evaluated. Screening results clearly show that Δ-enantiomer binding to D-DNA and Λ-enantiomer binding to L-DNA exhibits almost the same stabilization effect and binding affinity. In terms of G4 stabilization effect, iron metallohelices **3** displays the best chiral selectivity on antiparallel G4 DNA, one enantiomer stabilizing G4 DNA while the other even destabilizing G4 DNA. The binding affinity of Δ-**3** with D-G4 is nearly 70-fold higher than that of Λ-**3** with D-G4. Δ-**3** binding to D-G4 is following two-step binding and driven by a favourable enthalpy contribution to compensate the associated unfavourable entropy penalty. This work will advance current understanding of DNA chiral recognition and promote DNA-based chiral drug design.

Evolution of handedness is a characteristic hallmark of terrestrial life. Chiral recognition of biomolecules is a prerequisite in most biological processes.[1] As the carrier of genetic information, DNA possesses intrinsic chirality.[2] Unraveling the recognition mechanism of chiral species with DNA is an essential determinant for designing DNA-targeted drugs and developing DNA-based devices for chiral applications, including chiral sensing, chiral separation, asymmetric catalysis, and construction of molecular machine and logic devices.[3]

L-DNA, as the mirror-image counterpart of natural DNA (D-DNA), has identical physical characteristics to D-DNA but with opposite chirality.[4] Similar to D-DNA, L-DNA is polymorphic and can form various secondary structures, such as B-DNA, Z-DNA and G-quadruplex (G4) DNA, etc.[5] But distinctive from D-DNA, L-DNA is nuclease-resistant for its nonnative chirality and thus can be survived in biological environment.[6] L-DNA has been considered to be appealing replacement of D-DNA in nucleic acids-based in vivo diagnostic and therapeutic applications.[7] However, due to the inherent flexibility and conformation diversity of DNA, it is still unclear how enantiomeric compounds to recognize D-DNA and L-DNA. Are their recognitions following mirror-image dependence?

To this end, we choose G4 DNA as an example because G4 DNA is one of the most important noncanonical DNA with diverse conformations and distinct biofunctions.[8] Herein, 10 pairs of iron (Fe^{2+}) chiral barrel-like triplex metallohelices (metallohelices **1-10**), bearing both small molecular chemical features and helical nanometer size of a zinc-finger-like DNA-binding motif, binding to human telomeric G4 DNA (abbreviated as D-G4) and L-G4 have been screened and systematically compared with their enantioselectivity (Figure 1 and Figure S1). The screening results clearly indicated that Δ-enantiomer binding to D-G4 and Λ-enantiomer binding to L-G4 exhibited almost the same G4 DNA stabilization effect and binding affinity. In terms of G4 stabilization effect, metallohelices **3** displayed the best chiral selectivity on antiparallel G4 DNA, where one enantiomer stabilizing G4 while the other even destabilizing G4. To our knowledge, this is the first example to identify that it is mirror-image dependent for enantiomeric compounds to recognize D- and L-DNA.

CD studies verified that L-Tel22 (L-DNA with the same sequence as human telomeric D-Tel22) could form mirror-image structures of both antiparallel and hybrid D-G4 (Figure S2),[9] indicative of the formation of left-handed L-G4 (Figure 1B).[10] Next, screening of 10 pairs of metallohelices binding to D- and L-G4 was performed. [11] Binding constants of D- and L-G4 (antiparallel G4 in Na^+ buffer and hybrid G4 in K^+ buffer) with metallohelices were measured by UV-visible titration experiments.[12] For comparison, the binding constants were summarized in Figure 2A and 2B. Obviously, for all metallohelices, the binding constants of D-G4/Δ-enantiomers were nearly identical to that of L-G4/Λ-enantiomers. The same trend was found for L-G4/Δ-enantiomers and D-G4/Λ-enantiomers, no matter antiparallel or hybrid G4 used. Therefore, it can be concluded that the affinity of D/Δ and L/Λ pair is stronger than that of D/Λ and L/Δ pair, supporting the chiral selectivity, where left-handed Λ-enantiomer prefer left-handed L-G4, and right-handed Δ-enantiomer like right-handed D-G4.

The effects of metallohelices on the thermal stability of D- and L-G4 were next investigated (Figure S3-S6). DNA melting temperature change (ΔT_m) caused by metallohelices were shown in Figure 2C and 2D. Δ-enantiomers of metallohelices **1-3** displayed a better stabilization effect on both antiparallel and hybrid D-G4 than metallohelices **4-10**. Metallohelices **5-7**

[a] C. Zhao, A. Zhao, Prof. J. Ren, and Prof. X. Qu
Laboratory of Chemical Biology and State Key Laboratory of Rare Earth Resource Utilization, Changchun Institute of Applied Chemistry, Chinese Academy of Sciences,
Changchun, Jilin 130022, P. R. China
E-mail: xqu@ciac.ac.cn
[b] H. Song, Prof. P. Scott
Department of Chemistry, University of Warwick, Gibbet Hill Road, Coventry CV4 7AL, United Kingdom
[c] A. Zhao
University of Chinese Academy of Sciences,
Beijing 100039, P. R. China
[d] Dr. Hisae Tateishi-Karimata, and Prof. Naoki Sugimoto
FIBER, Konan University, 7-1-20 Minatojima-minamimachi, Chuo-ku, Kobe 650-0047, Japan

Supporting information for this article is given via a link at the end of the document.

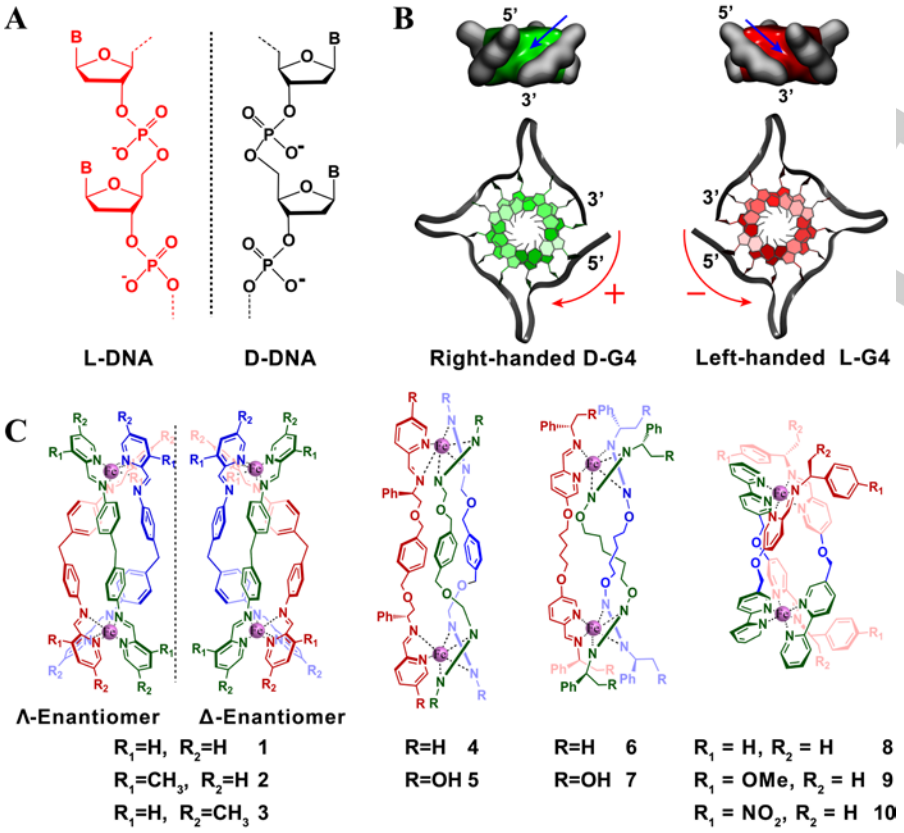

Figure 1. (A) Structures of D-DNA/L-DNA. (B) Schematic illustration of the directionality of the phosphate backbone of D-G4 and L-G4. (C) Structures of chiral iron metallohelices **1-10**.

exhibited a disappointing stabilization effect. These results implied that the structure of metallohelices, but not the electrostatic potential played a predominant role in stabilizing G4 DNA since all the metallohelices carried four positive charges. Thus, skeleton of metallohelices **1-3** (～1.8 nm in length, ～0.8 nm in diameter) may match better with G4 DNA (～1.4 nm length and ～ 1.1 nm width for G-quartet,) than other metallohelices. Also, by comparing metallohelices **2** and **3** with metallohelices **1**, it can be concluded that, after methyl substitution, their chiral selectivity changed dramatically, indicating that the substituent groups and the surroundings around Fe^{2+} of the metallohelices were crucial for their binding to G4 DNA. When D-G4 interacted with all metallohelices, Δ-enantiomers showed a stronger stabilization than Λ-enantiomers, implying that right-handed G4 prefers right-handed Δ-enantiomer, but not left-handed Λ-enantiomers. More importantly, ΔT_m of D/Δ pairs are comparable to that of L/Λ pairs, and D/Λ pairs are equal to L/Δ pairs, and this manner is concentration-independent (Figure S7).

Among the 10 pairs of iron metallohelices, metallohelices **3** (Λ-**3** and Δ-**3**) showed the best chiral selectivity on stabilizing antiparallel G4, where one enantiomer stabilizing G4 but the other even destabilizing G4. Further studies on different DNA secondary structures (dsDNA and i-motif DNA) clearly showed that metallohelices **3** was G4 selective binder (Figure S2 Table S1). Thus, focusing on metallohelices **3**, the detailed G4 binding mechanism was examined.

The effect of metallohelices **3** on the G4 DNA conformation was next studied. When treated D-G4 with Λ-**3**, D-G4 still adopted the antiparallel conformation (Figure 3A). In contrast, Δ-**3** induced the antiparallel D-G4 to hybrid D-G4 (Figure S8), similar with nickel (Ni^{2+}) metallohelices binding to D-G4 DNA.[13] When treated L-G4 with Λ-**3**, a nearly symmetric CD profile to that of D-G4/Δ-**3** pair was observed, indicating that Λ-**3** but not Δ-**3** can induce the antiparallel L-G4 to form hybrid L-G4. Further studies showed that only Δ-**3** but not Λ-**3** can induce single strand D-Tel22 to form G4 structure (Figure S9).

The binding properties of D-G4/L-G4 with Δ-**3**/Λ-**3** were next assessed by dialysis experiments.[14] In these assays, racemic samples containing Δ- and Λ-**3** were dialyzed against D- and L-G4, respectively. The enantiomer with higher affinity with D-G4 or L-G4 would come out of the dialysate and competitively bind to the preferred G4. In contrast, another enantiomer with lower binding affinity would be mainly retained in the dialysate. For L-G4 treated samples, Δ-**3** was detected in the corresponding dialysate, indicative of a stronger binding of L-G4 with Λ-**3**. In contrast, for D-G4 added samples, Λ-**3** was observed (Figure 3B). These results further confirmed the chiral selectivity of D-G4 for Δ-**3** and L-G4 for Λ-**3**, consistent well with the results of native gel electrophoresis experiments (Figure S10). More importantly, equimolar amounts of D-G4 and L-G4 lead to equal but opposite CD signals. Also, for sample containing equal amounts of D- and L-G4, no apparent CD signal was observed. These assays implied that G4 DNA can selectively capture their

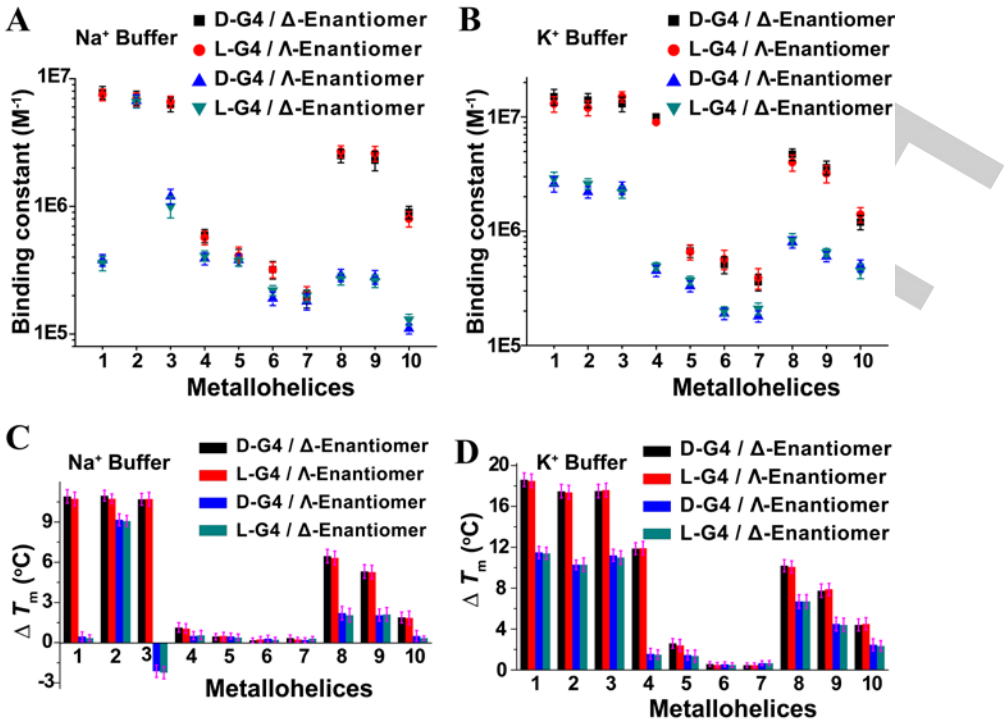

Figure 2. (A) Binding constants of antiparallel D-G4/L-G4 with enantiomers of metallohelices **1-10** in Na^+ buffer. (B) Binding constants of hybrid D-G4/L-G4 with enantiomers of metallohelices **1-10** in K^+ buffer. (C) Stabilization of antiparallel D-G4/L-G4 by enantiomers of metallohelices **1-10** in Na^+ buffer. (D) Stabilization of hybrid D-G4/L-G4 by enantiomers of metallohelices **1-10** in K^+ buffer. The results were from 3 independent experiments.

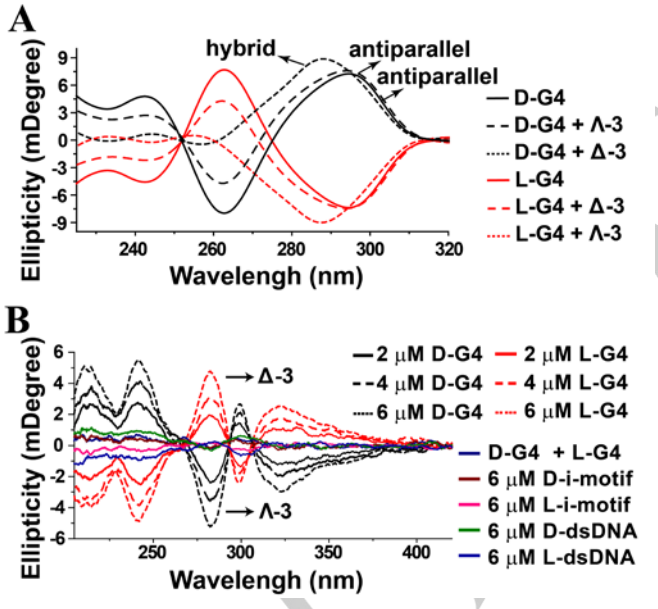

Figure 3. (A) CD spectra of D-G4 (black) or L-G4 (red) in the absence or presence of Δ-**3** and Λ-**3**. (B) CD spectra of the dialysate after dialysis of the racemic mixture of Δ-**3**/Λ-**3** against D-G4 (2-6 μM), L-G4 (2-6 μM), mixture of D-G4 and L-G4 (6 μM, respectively), D-i-motif (6 μM), L-i-motif (6 μM), D-dsDNA (6 μM) and L-dsDNA (6 μM), respectively. All assays were carried in 10 mM Tris-HCl, 100 mM NaCl, pH = 7.2 buffer.

preferred enantiomer from the racemic solution and the binding affinity of L-G4/Λ-**3** pair was nearly identical to that of D-G4/Δ-**3** pair, agreeing well with the affinity analysis.

To dissect more information on the binding of D-G4/L-G4 to Δ-**3**/Λ-**3**, we carried out kinetic studies by stopped-flow technique. For both D-G4/Δ-**3** and L-G4/Λ-**3** systems, the kinetic profiles displayed a biexponential behavior, inferring that there is a conformational transition from antiparallel G4 to hybrid G4 (Figure S11 and S12). Thus, a two-step binding mode was used to analyze the data. In contrast, D-G4/Λ-**3** and L-G4/Δ-**3** systems displayed a simple one step binding mode since no G4 DNA conformation transitions happened. Single (Eq. 1) or double-exponential equation (Eq. 2) was employed to elucidate the kinetics.[15]

$$k_{1obs} = k_1 C_M + k_{-1} \quad (1)$$

$$k_{2obs} = \frac{k_2 C_M}{K_1 + C_M} + k_{-2} \quad (2)$$

where k_{1obs} is the observed rate of the fast phase; k_{2obs} is the observed rate of the slow phase; C_M is metallohelices concentration; k_1 and k_{-1} are the association rate and dissociation rate of the fast phase; k_2 and k_{-2} are the association rate and dissociation rate of the slow phase; K_1 is the association constant of the fast phase and $K_1 = k_1/k_{-1}$.

The reaction parameters of different steps were shown in Figure 4A (Figure S13). Clearly, mirror-image pairs (D/Δ and L/Λ pair, D/Λ and L/Δ pair) exhibited almost the same kinetic parameters, which provided the most compelling evidence that the recognition processes of D- and L-G4 by Δ- and Λ-**3** were mirror-imaged. The parameters also well explained the chiral selectivity of Δ-**3** and Λ-**3**. Taking D-G4 as an example, Λ-**3** binding with D-G4 yielded an equilibrium association constant K of $1.5\pm0.2\times10^5$ M^{-1}. In contrast, Δ-**3** adopted a two-step binding mode with D-G4 where Δ-**3** binding fast to D-G4 was followed by a slow isomerization of the complex, and an overall equilibrium

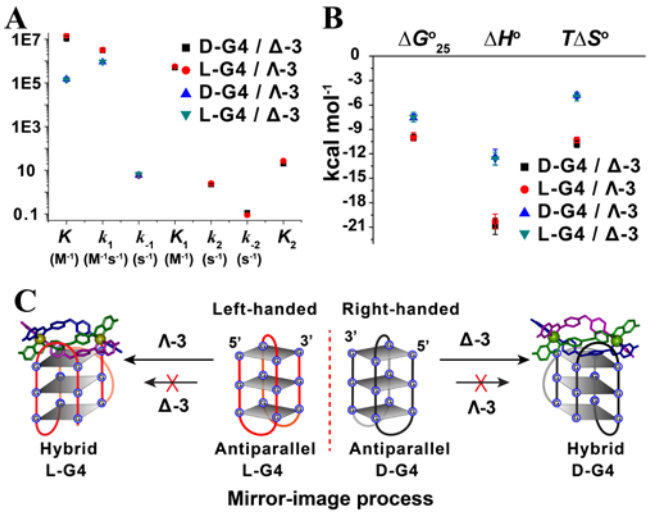

Figure 4. (A) Kinetic parameters of Δ-**3**/Λ-**3** with D-G4/L-G4. The parameters were obtained from stopped-flow studies. The experiments were performed in 10 mM Tris-HCl, 100 mM NaCl, pH = 7.2 buffer. (B) Thermodynamic parameters of D-G4/L-G4 DNA binding with Δ-**3**/Λ-**3**. Data were obtained from ITC assays. ΔH^o was directly obtained from ITC. ΔG^o_{25} was obtained from the relation ΔG^o = -RTln*Ka*. $T\Delta S^o$ obtained from the relation $T\Delta S^o = \Delta H^o - \Delta G^o$. Assays were performed in 10 mM Tris, 100 mM NaCl, pH = 7.2 buffer. The values were the average of 3 independent measurements. (C) Representative illustration of the mirror-image recognition process of G4 DNA by chiral metallohelices. Black represents the right-handed D-G4 and red represents the left-handed L-G4.

association constant *K* was determined to be 1.1×10^7 M^{-1}, 73-fold higher than that of Λ-**3**. This result was well coincidental with the above affinity analysis. It also should be noted that, K_1 for Δ-**3** binding to D-G4 was just 3.4-fold higher than that of Λ-**3** binding to D-G4, thus the stronger binding affinity for Δ-**3** was mainly assigned to the second step of conformational isomerization.

To further elucidate the molecular mechanism of D-G4/L-G4 binding with Δ-**3**/Λ-**3**, we analyze their binding enthalpy and entropy change by ITC measurements (Figure S14 and Table S2). Clearly, mirror-image pairs exhibited almost the same thermodynamics parameters, as shown by the overlapped red (D-G4/Δ-**3**) and black (L-G4/Λ-**3**) points, blue (D-G4/Λ-**3**) and green (L-G4/Δ-**3**) points in Figure 4B. These results provided further evidence that the recognition processes of D- and L-G4 by Δ- and Λ-**3** was mirror-image dependent (Figure 4C). Also, the parameters were in good agreement with the chiral selectivity of Δ-**3** and Λ-**3**. Taking D-G4 as an example, a larger free energy change was observed for binding with Δ-**3** than that of Λ-**3**, which explained the stronger stabilization of Δ-**3** for D-G4. Moreover, for both Δ-**3** and Λ-**3**, the binding process was facilitated by a favorable enthalpy contribution to compensate the associated unfavorable entropy penalty. However, Δ-**3** exhibited a more favorable enthalpy contribution than Λ-**3**, which resulted in more favorable free energy change for D-G4/Δ-**3** binding.

In summary, we have screened 10 pairs of iron triplex metallohelices binding to enantiomeric G-quadruplex DNA. The results clearly show mirror-image dependence for Δ- or Λ-enantiomer binding to D- or L-DNA. In terms of G4 stabilization effect, iron metallohelices **3** displays the best chiral selectivity on antiparallel G4 DNA, Δ-enantiomer stabilizing G4 DNA while Λ-enantiomer even destabilizing G4 DNA. Δ-**3** binding to D-G4 is driven by a favorable enthalpy contribution to compensate the associated unfavorable entropy penalty. To our knowledge, this is the first example to show mirror-image dependence for enantiomeric compounds binding to D- and L-DNA. This will advance current understanding of chiral ligand-DNA recognition and promote DNA-based chiral drug design.

Acknowledgements

Financial support was provided by NSFC (21431007, 21533008, 21572216, 21820102009, 21871249), Key Program of Frontier of Sciences, CAS QYZDJ-SSW-SLH052, and JSPS KAKENHI (Grant No. JP17H06351).

Keywords: Mirror-image • G-quadruplex DNA • Metallohelices • Enantiomer • Chiral recognition

[1] a) R. Bentley, *Chem. Soc. Rev.* **2005**, *34*, 609-624; b) H. Caner, E. Groner, L. Levy, I. Agranat, *Drug Discov. Today* **2004**, *9*, 105-110; c) J. Gal, *Chirality* **2012**, *24*, 959-976.

[2] D. D'Alonzo, A. Guaragna, G. Palumbo, *Chem. Biodivers.* **2011**, *8*, 373-413.

[3] a) R. Corradini, S. Sforza, T. Tedeschi, R. Marchelli, *Chirality* **2007**, *19*, 269-294; b) Z. Wang, W. Xu, L. Liu, T. F. Zhu, *Nat. Chem.* **2016**, *8*, 698-704; c) R. C. Milton, S. C. Milton, S. B. Kent, *Science* **1992**, *256*, 1445-1448; d) L. Tohala, F. Oukacine, C. Ravelet, E. Peyrin, *Anal. Chem.* **2015**, *87*, 5491-5495; e) C. Lin, Y. Ke, Z. Li, J. H. Wang, Y. Liu, H. Yan, *Nano Lett.* **2009**, *9*, 433-436; f) G. Roelfes, B. L. Feringa, *Angew. Chem. Int. Ed.* **2005**, *44*, 3230-3232; g) T. A. Feagin, D. P. V. Olsen, Z. C. Headman, J. M. Heemstra, *J. Am. Chem. Soc.* **2015**, *137*, 4198-4206; h) M. You, G. Zhu, T. Chen, M. J. Donovan, W. Tan, *J. Am. Chem. Soc.* **2015**, *137*, 667-674.

[4] I. Tazawa, S. Tazawa, L. M. Stempel, P. O. Ts'o, *Biochemistry* **1970**, *9*, 3499-3514.

[5] P. L. Tran, R. Moriyama, A. Maruyama, B. Rayner, J. L. Mergny, *Chem. Commun.* **2011**, *47*, 5437-5439.

[6] K. P. Williams, X. H. Liu, T. N. Schumacher, H. Y. Lin, D. A. Ausiello, P. S. Kim, D. P. Bartel, *Proc. Natl. Acad. Sci. USA* **1997**, *94*, 11285-11290.

[7] a) D. Eulberg, S. Klussmann, *Chembiochem.* **2003**, *4*, 979-983; b) E. Wyszko, M. Szymanski, H. Zeichhardt, F. Muller, J. Barciszewski, V. A. Erdmann, *PloS one* **2013**, *8*, e54741; c) Y. Kim, C. J. Yang, W. Tan, *Nucleic Acids Res.* **2007**, *35*, 7279-7287.

[8] a) J. L. Huppert, *Chem Soc Rev* **2008**, *37*, 1375-1384; b) G. Biffi, D. Tannahill, J. McCafferty, S. Balasubramanian, *Nat. Chem.* **2013**, *5*, 182-186; c) T. Endoh, Y. Kawasaki, N. Sugimoto, *Angew. Chem. Int. Ed.* **2013**, *52*, 5522-5526; d) X. M. Li, K. W. Zheng, J. Y. Zhang, H. H. Liu, Y. D. He, B. F. Yuan, Y. H. Hao, Z. Tan, *Proc. Natl. Acad. Sci. USA* **2015**, *112*, 14581-14586. e) Y. Xu, *Chem. Soc. Rev.* **2011**, *40*, 2719-2740; f) R. J. O'Sullivan, J. Karlseder, *Nat. Rev. Mol. Cell. Biol.***2010**, *11*, 171-181; g) W. J. Chung, B. Heddi, E. Schmitt, K. W. Lim, Y. Mechulam, A. T. Phan, *Proc. Natl. Acad. Sci. USA* **2015**, *112*, 2729-2733; h) M. Read, R. J. Harrison, B. Romagnoli, F. A. Tanious, S. H. Gowan, A. P. Reszka, W. D. Wilson, L. R. Kelland, S. Neidle, *Proc. Natl. Acad. Sci. USA* **2001**, *98*, 4844-4849; i) M.-Y. Kim, H. Vankayalapati, K. Shin-ya, K. Wierzba, L. H. Hurley, *J. Am. Chem. Soc.* **2002**, *124*, 2098-2099; j) J. Abraham Punnoose, Y. Ma, Y. Li, M. Sakuma, S. Mandal, K. Nagasawa, H. Mao, *J. Am. Chem. Soc.* **2017**, *139*, 7476-7484.

[9] a) Y. Wang, D. J. Patel, *Structure* **1993**, *1*, 263-282; b) A. Ambrus, D. Chen, J. X. Dai, T. Bialis, R. A. Jones, D. Z. Yang, *Nucleic Acids Res.* **2006**, *34*, 2723-2735; c) A. T. Phan, V. Kuryavyi, K. N. Luu, D. J. Patel, *Nucleic Acids Res.* **2007**, *35*, 6517-6525.

[10] R. del Villar-Guerra, O. Trent John, B. Chaires Jonathan, *Angew. Chem. Int. Ed.* **2018**, *57*, 7171-7175.

[11] a) M. J. Hannon, C. L. Painting, A. Jackson, J. Hamblin, W. Errington, *Chem. Commun.* **1997**, 1807-1808. b) G. Clarkson, D. J. Fox, P. Gurnani, S. E. Howson, R. M. Phillips, D. I. Roper, D. H. Simpson, P. Scott, S. E. Howson, A. Bolhuis, V. Brabec, G. J. Clarkson, J. Malina, A. Rodger, P. Scott, *Nat. Chem.* **2011**, *4*, 31-36. c) Faulkner, A. D.; Kaner, R. A.; Abdallah, Q. M. A.; Clarkson, G.; Fox, D. J.; Gurnani, P.; Howson, S. E.; Phillips, R. M.; Roper, D. I.; Simpson, D. H.; Scott, P. *Nat. Chem.*

2014, *6*, 797. d) Zhao, C.; Geng, J.; Feng, L.; Ren, J.; Qu, X. *Chem. Eur. J.* **2011**, *17*, 8209-8215.

[12] a) R. B. Nair, E. S. Teng, S. L. Kirkland, C. J. Murphy, *Inorg. Chem.* **1998**, *37*, 139-141; b) M. T. Carter, M. Rodriguez, A. J. Bard, *J. Am. Chem. Soc.* **1989**, *111*, 8901-8911.

[13] a) H. Yu, X. Wang, M. Fu, J. Ren, X. Qu, *Nucleic Acids Res.* **2008**, *36*, 5695-5703; b) A. Zhao, S. E. Howson, C. Zhao, J. Ren, P. Scott, C. Wang, X. Qu, *Nucleic Acids Res.* **2017**, *45*, 5026-5035; c) H. Qin, C. Zhao, Y. Sun, J. Ren, X. Qu, *J. Am. Chem. Soc.* **2017**, *139*, 16201-16209.

[14] X. Qu, J. O. Trent, I. Fokt, W. Priebe, J. B. Chaires, *Proc. Natl. Acad. Sci. U S A* **2000**, *97*, 12032-12037.

[15] a) C. Bazzicalupi, S. Biagini, A. Bianchi, T. Biver, A. Boggioni, C. Giorgi, P. Gratteri, M. Malavolti, F. Secco, B. Valtancoli, M. Venturini, *Dalton Trans.* **2010**, *39*, 9838-9850; b) S. M. Patrick, J. J. Turchi, *J. Biol. Chem.* **2001**, *276*, 22630-22637.

Table of Contents

COMMUNICATION

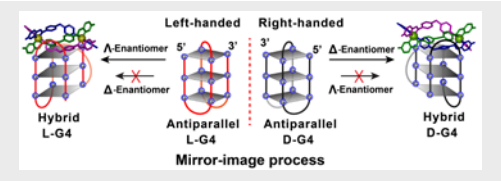

Chiral recognition of DNA plays crucial roles in many DNA-relevant events. 10 pairs of iron helical metallohelices binding to enantiomeric G-quadruplex DNA have been screened. The results clearly show mirror-image dependence for Δ- or Λ-enantiomer binding to D-DNA or L-DNA.

*Chuanqi Zhao, Hualong Song, Peter Scott, Andong Zhao, Hisae Tateishi-Karimata, Naoki Sugimoto, Jinsong Ren and Xiaogang Qu**

Page No. – Page No.

Mirror-image Dependence: Targeting Enantiomeric G-quadruplex DNA by 10 Pairs of Triplex Metallohelices